Electronic Supplementary Information

How does the single unit monomer insertion technique promote kinetic analysis of activation and initiation in photo-RAFT process?

Lei Zhang, Ruizhe Liu, Zixuan Huang, Jiangtao Xu*

Centre for Advanced Macromolecular Design, School of Chemical Engineering, UNSW Sydney, NSW 2052, Australia

1. Materials and instrument

1.1 Materials

N-phenylmaleimide (PMI, 97%), *N*-(2-hydroxyethyl)maleimide (HEMI, 97%), *trans*-anethole (Ane, 99%) and 5,10,15,20-tetraphenyl-21H,23H-porphine zinc (ZnTPP, 98%) were purchased from Sigma-Aldrich and used as received. Acrylonitrile (ACN, 99%), methyl acrylate (MA, 99%), *N*, *N*-Dimethylacetamide (DMA, 99%) were purchased from Sigma-Aldrich and purified with a column of basic alumina before use. (2-cyanopropan-2-yl) carbonotrithioate (CPBTC) and *n*-butyl benzyl trithiocarbonate (BBTC) were lab-synthesized. Dimethyl sulfoxide (DMSO), chloroform, n-hexane, ethyl acetate, were purchased from Ajax Chemical and used as received.

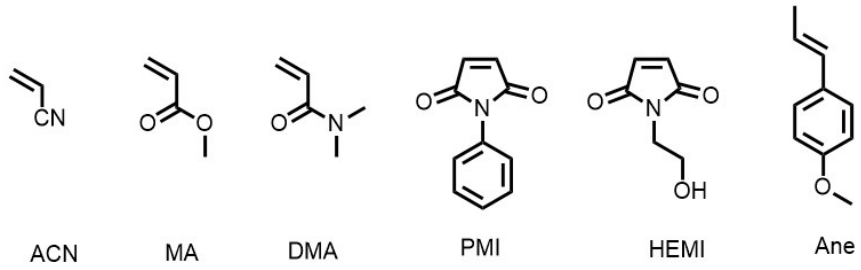

Figure S1. Chemical structures of monomers used in this study.

1.2 Instrument

Nuclear magnetic resonance (NMR) spectroscopy was carried out on a Bruker Advance III (400 MHz) with SampleXpress operating at 400 MHz for ^{1}H, ^{13}C, ^{1}H-^{13}C HMBC and ^{1}H-^{13}C HSQC using $CDCl_3$ or DMSO-d_6 as solvent and tetramethylsilane (TMS) as a reference. The data obtained was reported as chemical shift (δ) measured in ppm downfield from TMS.

Column chromatography was used for product purification. Biotage® (Isolera One) automated flash chromatography with SNAP Ultra cartridges and ZIP Sphere cartridges was employed in the purification process.

Photo reactor was irradiated by LED RGB strip light rearranged in a glass bath with a diameter of 12 cm (red light: λ_{max} = 635 nm, 0.23 mW cm^{-2}; green light: λ_{max} = 530 nm, 0.36 mW cm^{-2}; blue light: λ_{max} =

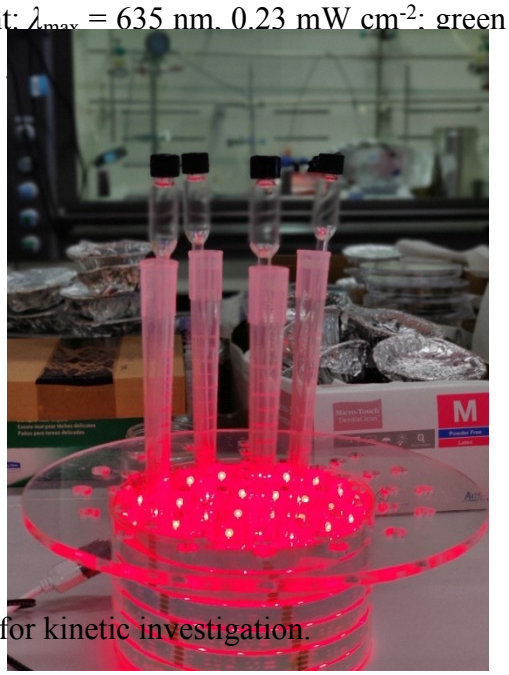

Figure S2. LED light used for kinetic investigation.

2. Synthesis and characterization of RAFT agents 1, 2 and 3

2.1 Synthesis of CPBTC-Ane (1)

CPBTC (100 mg, 0.43 mmol), Ane (1270 mg, 0.86 mmol) was dissolved in 4 mL toluene in a 21 mL glass vial. The vial was then sealed with a rubber septum and the reaction solution was degassed with nitrogen for 20 min. Then the reaction mixture was irradiated under blue LED light (0.36 mW cm^{-2}) at room temperature. After 40 h, the solvent toluene was evaporated and the crude product was subjected to column chromatography using silica gel as stationary phase and *n*-hexane/ethyl acetate (40/1 to 20/1, v/v) as gradient eluent. The final product was yellow liquid (yield: 69%).

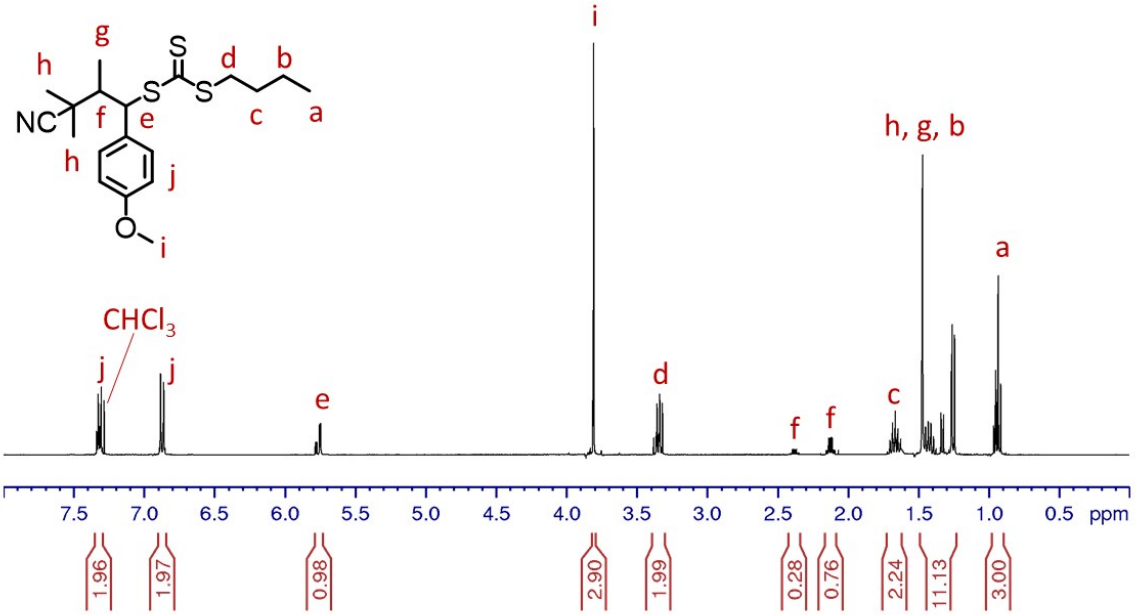

Figure S3. ^{1}H NMR (400 MHz, $CDCl_3$) spectrum of CPBTC-Ane (**1**).

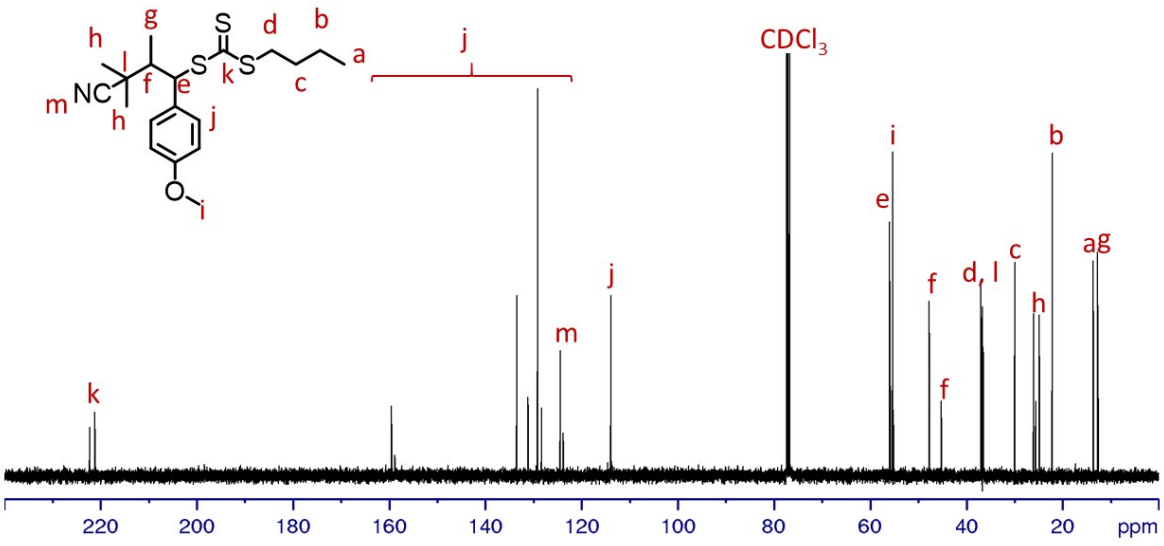

Figure S4. ^{13}C NMR (100 MHz, $CDCl_3$) spectrum of CPBTC-Ane (**1**).

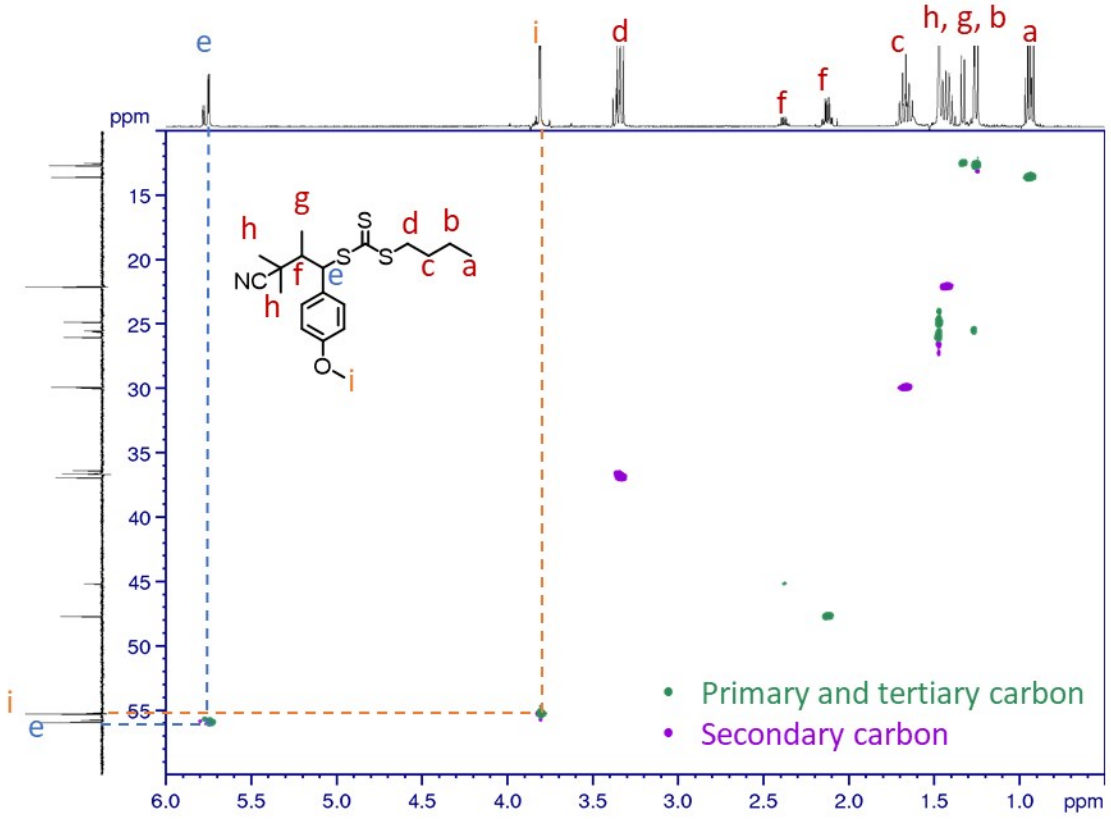

Figure S5. Enlarged ^{1}H-^{13}C HSQC ($CDCl_3$) spectrum of CPBTC-Ane (**1**).

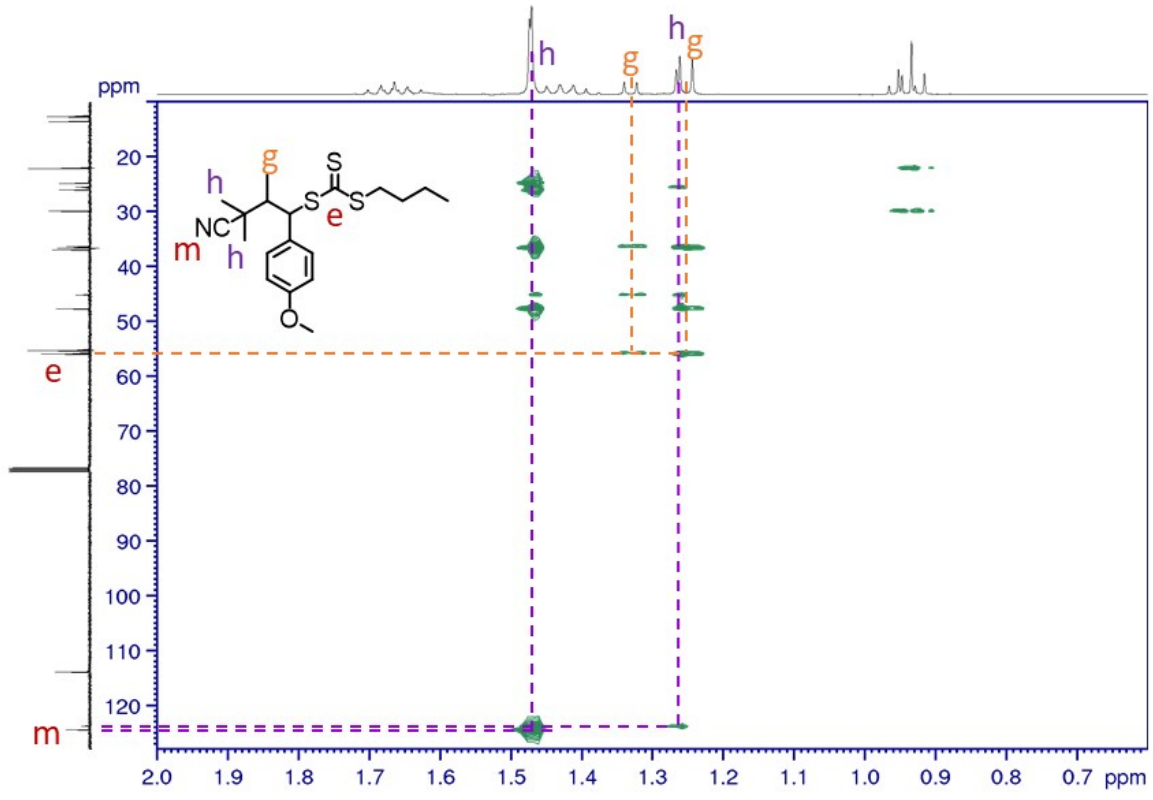

Figure S6. Enlarged ^{1}H-^{13}C HMBC ($CDCl_3$) of CPBTC-Ane (**1**).

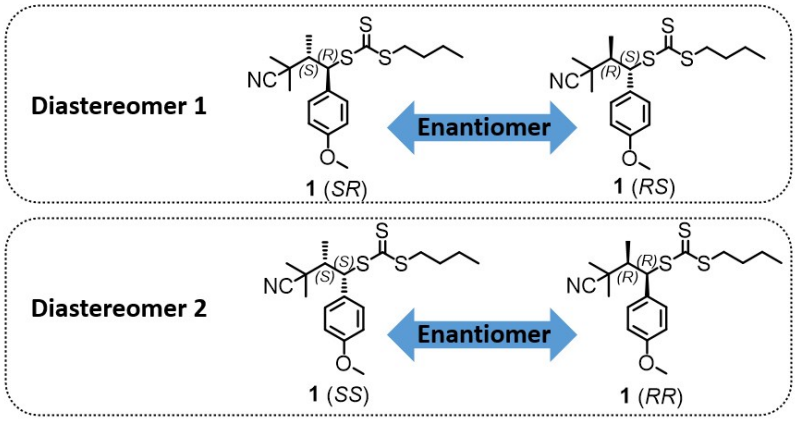

Figure S7. Different isomers of CPBTC-Ane (**1**) (Each of the diastereomers is assumed to comprise a pair of enantiomers with identical NMR spectra)

2.2 Synthesis of CPBTC-ACN-Ane (2)

Synthesis of CPBTC-ACN

CPBTC (210 mg, 0.9 mmol) and ACN (238 mg, 4.5 mmol) was dissolved in 4.4 mL toluene in a 21 mL vial. The vial was then sealed with a rubber septum and the reaction solution was degassed with nitrogen for 20 min. Then the reaction mixture was irradiated under green LED light (0.36 mW cm^{-2}) at room temperature. After 9 h, the solvent toluene was evaporated and the crude product was subjected to column chromatography using silica gel as stationary phase and *n*-hexane/ethyl acetate (10/0 to 10/1, v/v) as gradient eluent. The final product was yellow liquid (yield: 65%).

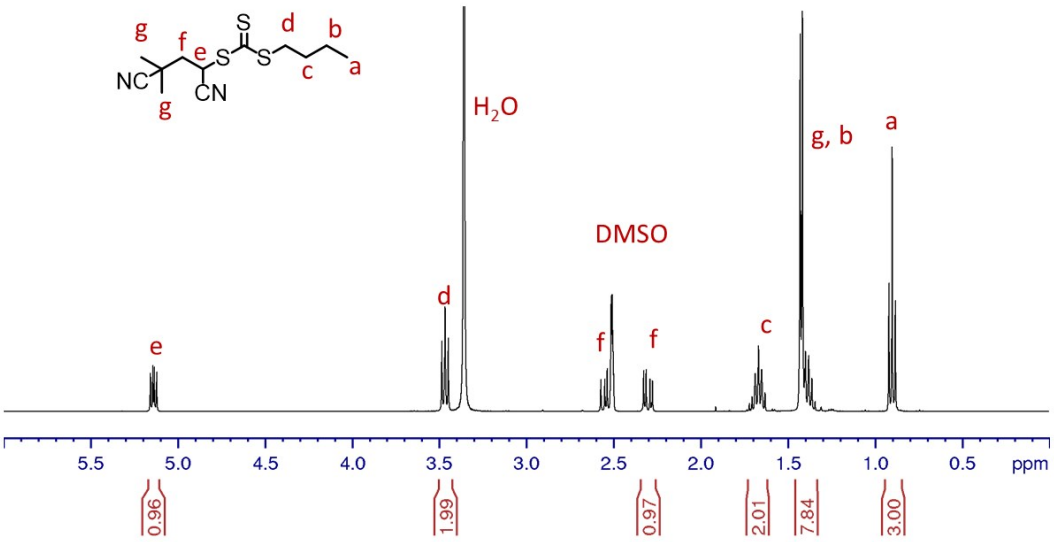

Figure S8. ^{1}H NMR (400 MHz, DMSO-d_6) spectrum of CPBTC-ACN.

Synthesis of CPBTC-ACN-Ane (2)

CPBTC-ACN (60 mg, 0.21 mmol), Ane (311 mg, 2.1 mmol) and ZnTPP (1.4 mg, 0.0021 mmol) was resolved in 6.5 mL DMSO in a 21 mL vial. The vial was sealed with a rubber septum and the reaction solution was degassed with nitrogen for 20 min. Then the reaction mixture was irradiated under red LED light (0.23 mW cm^{-2}) at room temperature. After 9h, 15 mL $CHCl_3$ was added to the reaction solution and 15 mL deionized water was also added to extract DMSO from $CHCl_3$. The extracting step was repeated three times and the organic phase was collected. The solvent $CHCl_3$ was evaporated and the crude product was purified by column chromatography using silica gel as stationary phase and n-hexane/ethyl acetate (50/1 to 5/1, v/v) as gradient eluent. The final product was yellow oil (yield:96%).

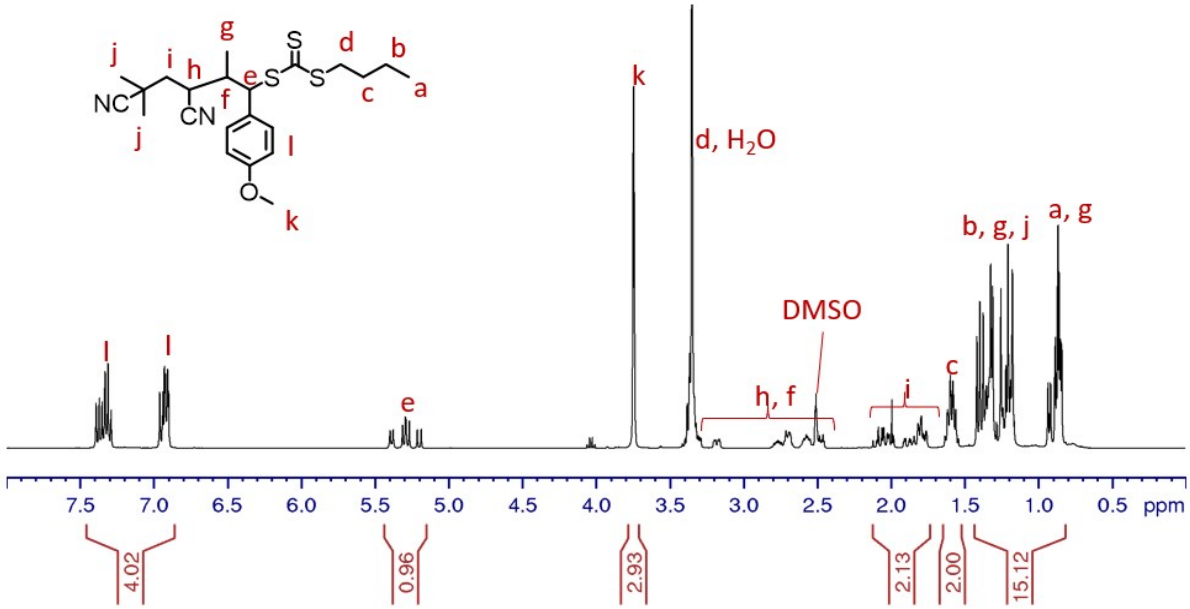

Figure S9. ^{1}H NMR (400 MHz, DMSO-d_6) of purified CPBTC-ACN-Ane (**2**).

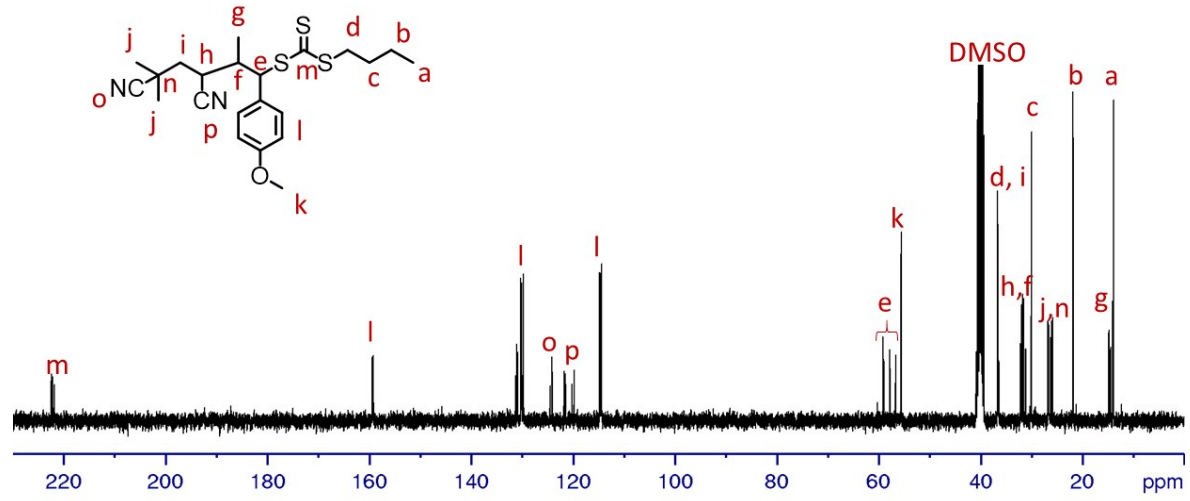

Figure S10. ^{13}C NMR (100 MHz, DMSO-d_6) of purified CPBTC-ACN-Ane (**2**).

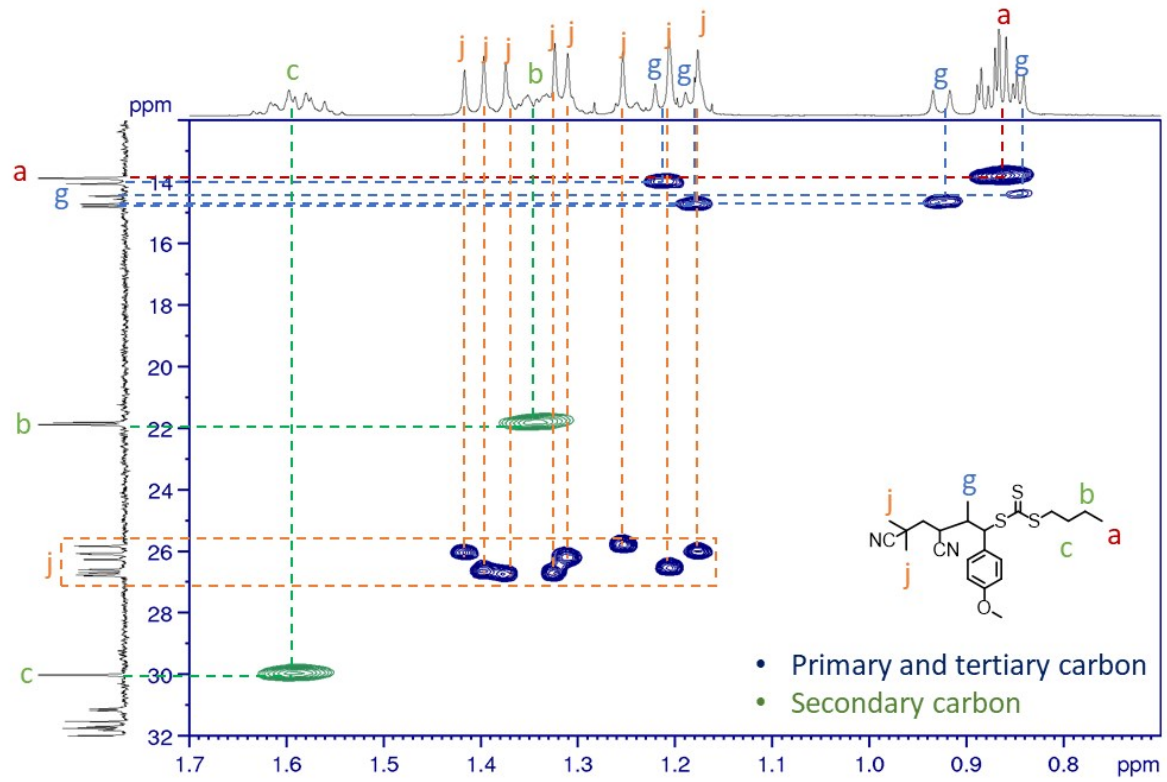

Figure S11. Enlarged ^{1}H-^{13}C HSQC (DMSO-d_6) of purified CPBTC-ACN-Ane (**2**).

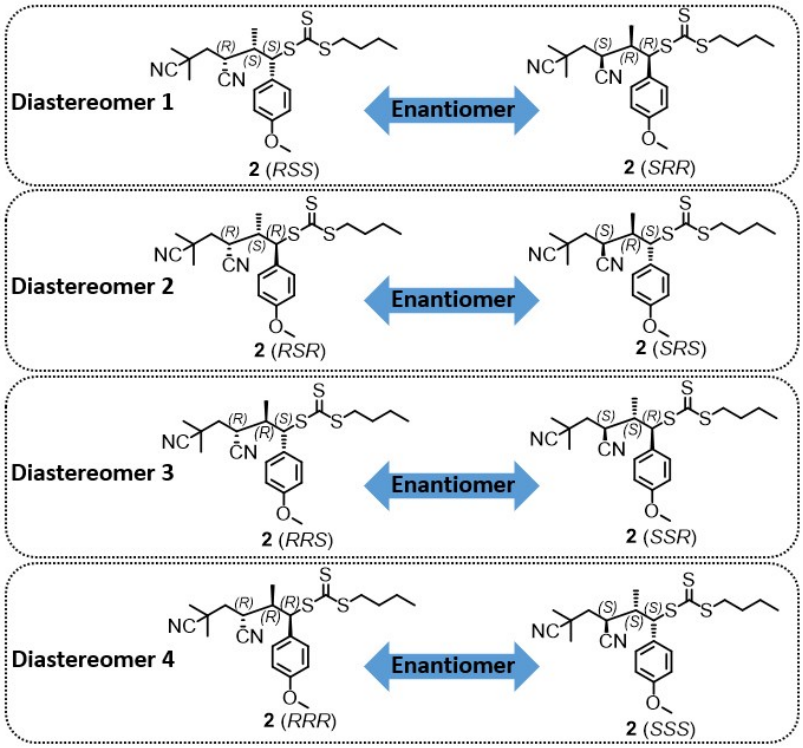

Figure S12. Different isomers of CPBTC-ACN-Ane (**2**). Each diastereomer is assumed to comprise a pair of enantiomers which have identical NMR spectra.

2.3 Synthesis of BBTC-PMI-Ane (3)

Synthesis of BBTC-PMI

BBTC (500 mg, 1.95 mmol), PMI (338 mg, 1.95 mmol) and ZnTPP (6.6 mg, 0.0098 mmol) was dissolved in 15 mL DMSO in a 21mL vial. The vial was sealed with a rubber septum and the reaction solution was degassed with nitrogen for 20 min. Then the reaction mixture was irradiated under red LED light (0.23 mW cm^{-2}) at room temperature. After 24h, 30 mL $CHCl_3$ was added to the reaction solution and 30 mL deionized water was also added to extract DMSO from $CHCl_3$. The extracting step was repeated three times and the organic phase was collected. The solvent $CHCl_3$ was evaporated and the crude product was purified by column chromatography using silica gel as stationary phase and *n*-hexane/ethyl acetate (100/1 to 15/1, v/v) as gradient eluent. The final product was yellow oil (yield: 55%).

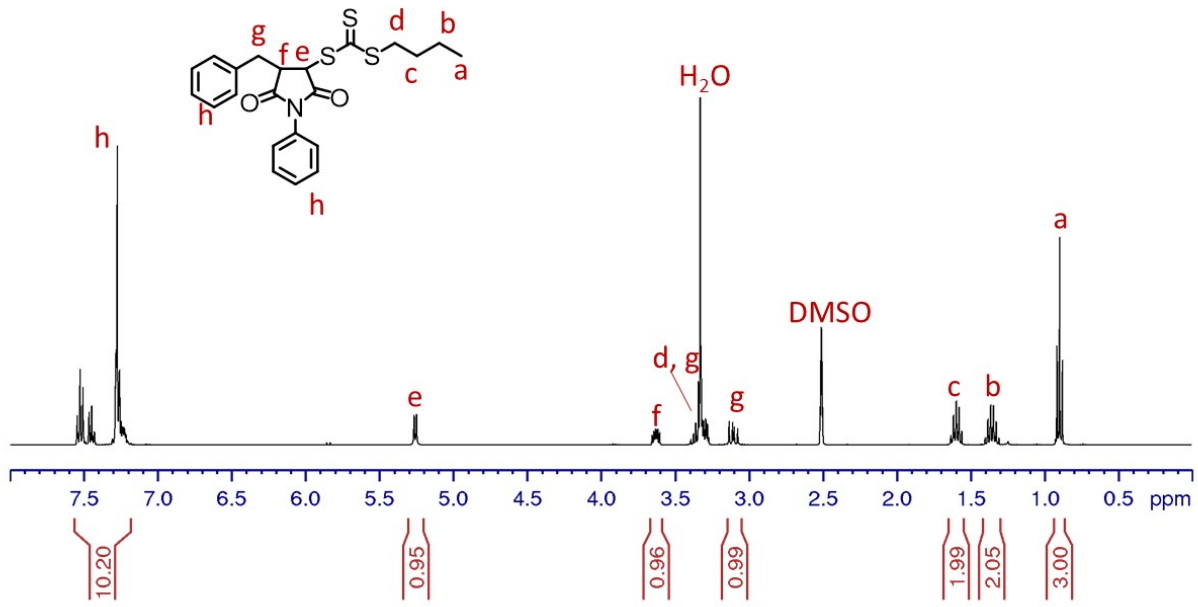

Figure S13. ^{1}H NMR (400 MHz, DMSO-d_6) of BBTC-PMI.

Synthesis of BBTC-PMI-Ane (3)

BBTC-PMI (250 mg, 0.58 mmol), Ane (430 mg, 2.9 mmol) and ZnTPP (4 mg, 0.0058 mmol) was dissolved in 10 mL DMSO. The vial was sealed with a rubber septum and the reaction solution was degassed with nitrogen for 20 min. Then the reaction mixture was irradiated

under red LED light (0.23 mW cm^{-2}) at room temperature. After 10 h, 20 mL $CHCl_3$ was added to the reaction solution and 20 mL deionized water was also added to extract DMSO from $CHCl_3$. The extracting step was repeated three times and the organic phase was collected. The solvent $CHCl_3$ was evaporated and the crude productcrude product was purified by column chromatography using silica gel as stationary phase and *n*-hexane/ethyl acetate (50/1 to 10/1, v/v) as gradient eluent. The final product was yellow solid (yield: 51%).

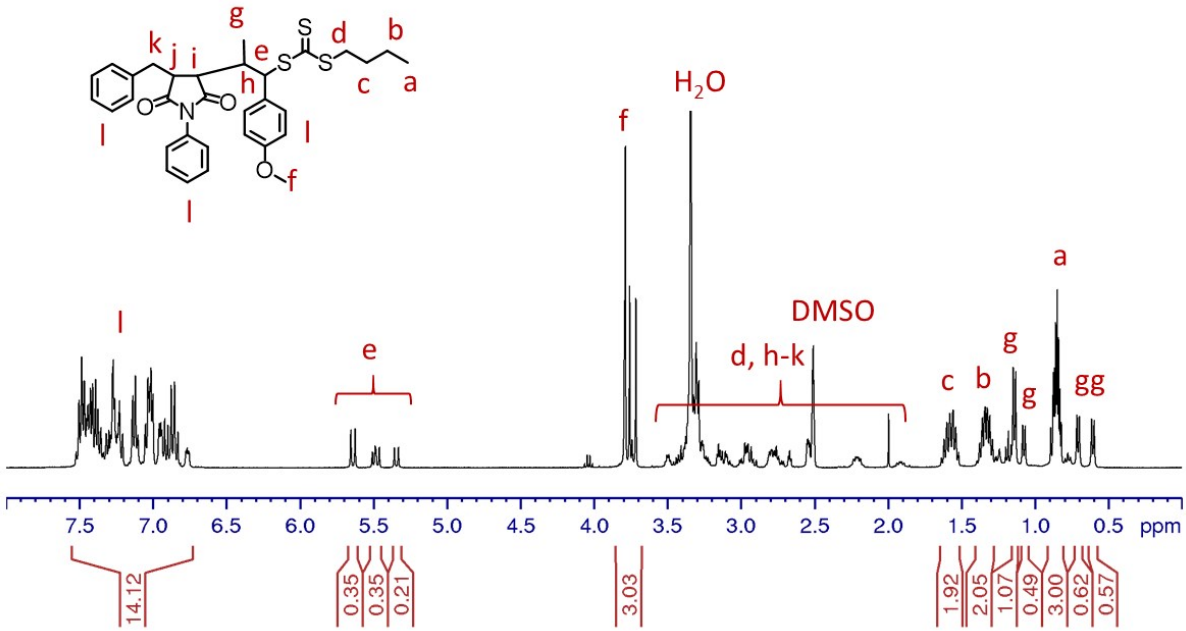

Figure S14. ^{1}H NMR (400 MHz, DMSO-d_6) of BBTC-PMI-Ane (**3**).

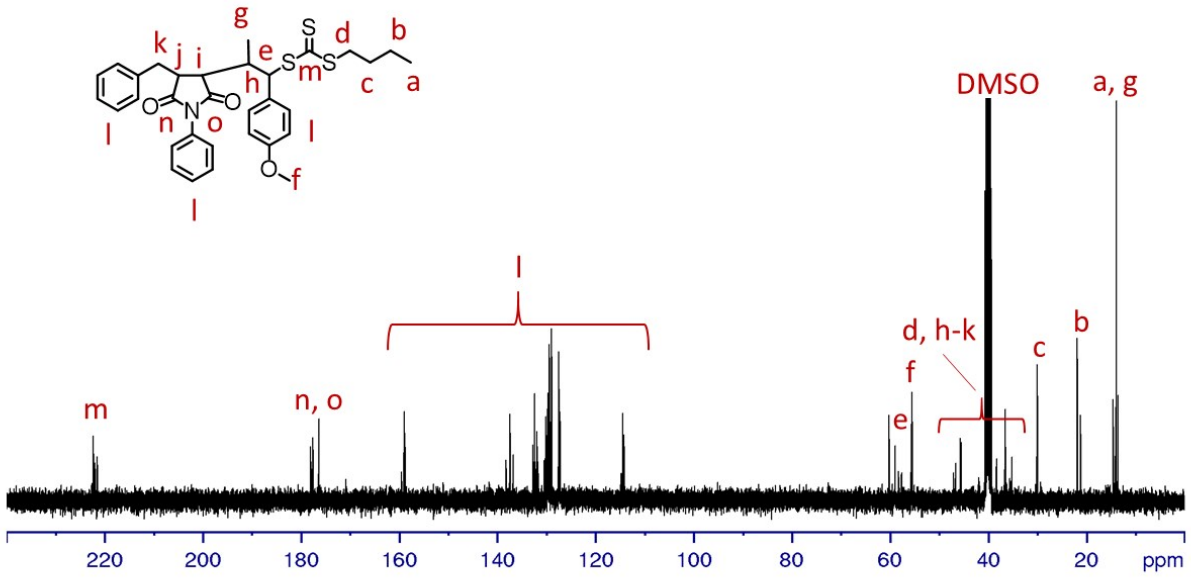

Figure S15. ^{13}C NMR (100 MHz, DMSO-d_6) of BBTC-PMI-Ane (**3**).

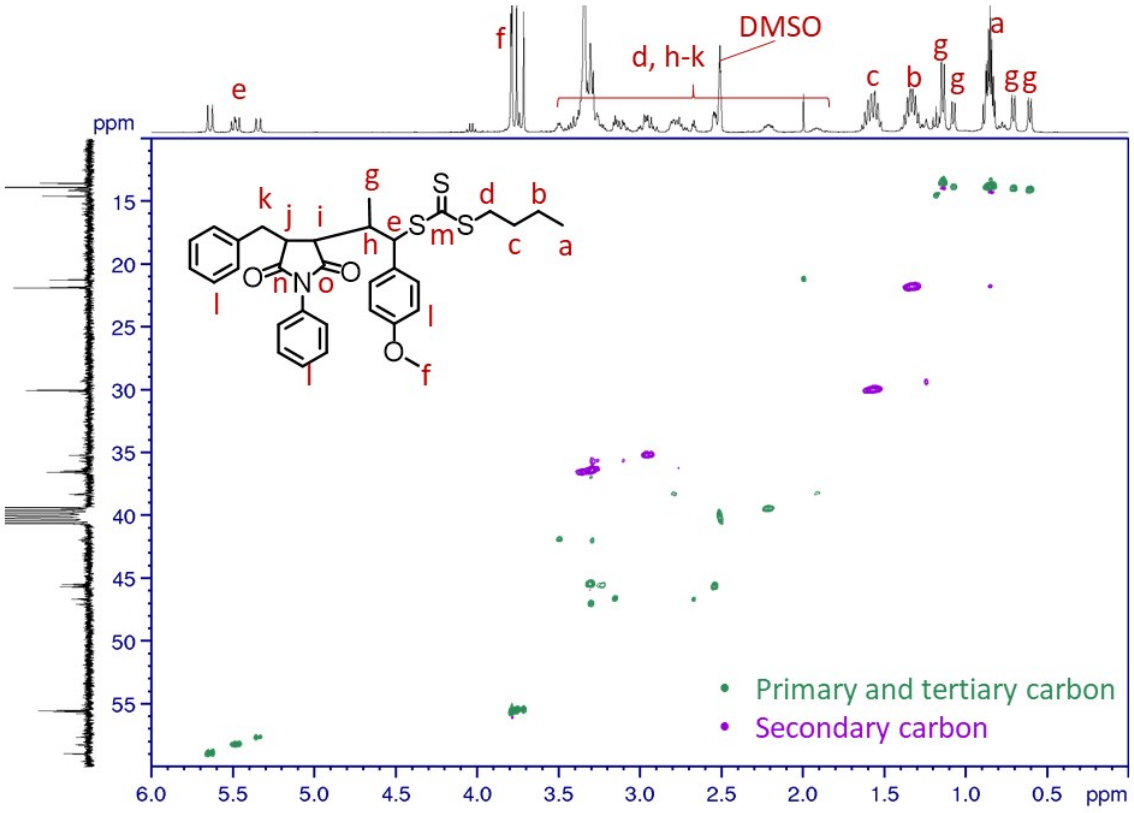

Figure S16. Enlarged ^{1}H-^{13}C HSQC NMR (DMSO-d_6) of BBTC-PMI-Ane (**3**).

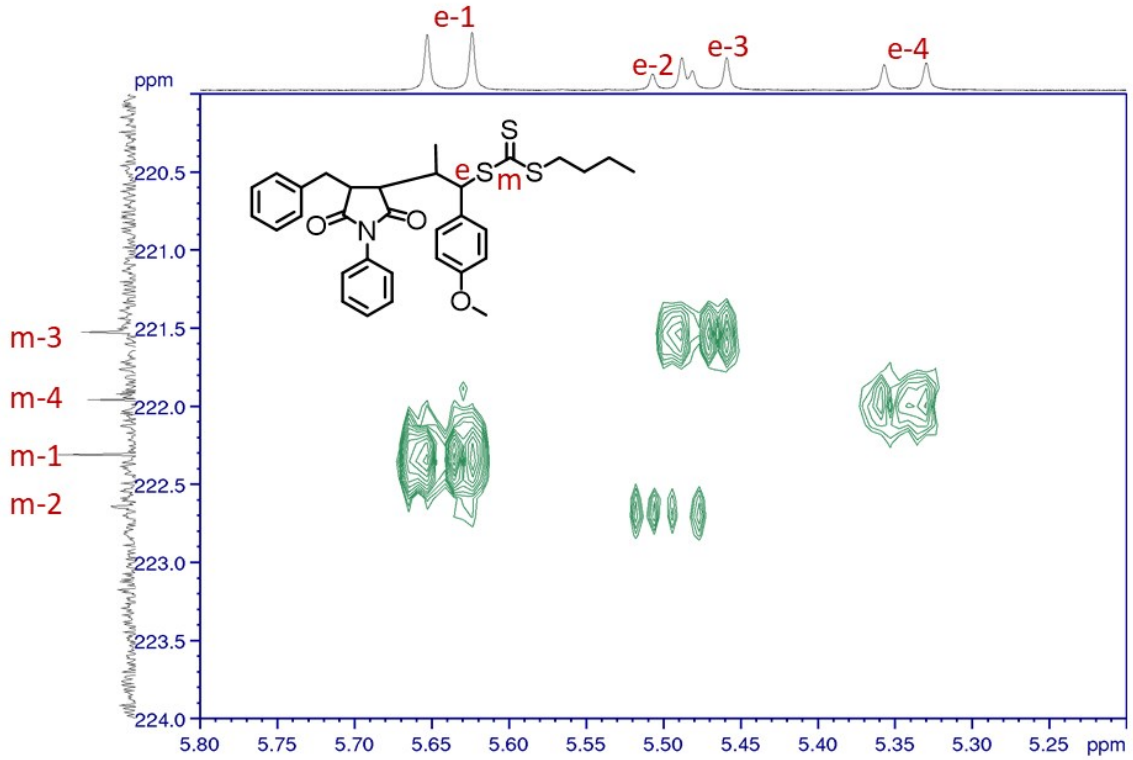

Figure S17. Enlarged ^{1}H-^{13}C HMBC (DMSO-d_6) of BBTC-PMI-Ane (**3**) showing long distance correlation of the proton e and the carbon m and also the presence of four diastereomers (shown as follows) of the compound.

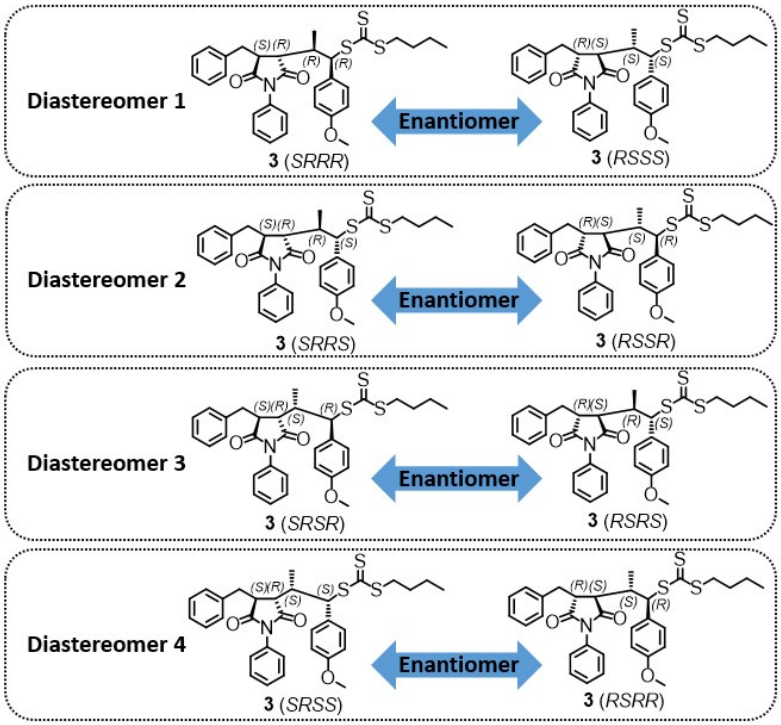

Figure S18. Different isomers of BBTC-PMI-Ane (**3**).

3. Kinetic investigation of three RAFT agents reacting with identical monomers

The SUMI reactions between RAFT agents with various monomers, PMI, HEMI, ACN, MA and DMA was studied. The photo-SUMI reaction solution was prepared according to the following formula: DMSO-d_6 as solvent, [RAFT]:[Monomer]:[ZnTPP] = 1:1:0.01, [RAFT] = 0.025 mol L^{-1}. Each reaction solution was transferred to a screw-cap NMR tube, sealed and degassed by nitrogen for 10 min. The reaction mixture was then irradiated under red LED strip (0.23 mW cm^{-2}) at room temperature. After different irradiation time (0, 3 and 6 h), the NMR tube was transferred into the instrument to collect ^{1}H NMR spectrum. After that, the molar ratio of [ACN]:[RAFT] was changed to 10:1 and the same test was performed.

The kinetic study experiment was carried out in DMSO-d_6 by monitoring RAFT agent conversion using online ^{1}H NMR spectroscopy. For PMI insertion study, RAFT agent, PMI, ZnTPP was dissolved in DMSO-d_6 to obtain 600 μL solution with the molar ratio of [RAFT]:[PMI]:[ZnTPP] = 1:1:0.01 and [RAFT] = 0.025 mol L^{-1}. Then the solution was transferred to three screw-cap NMR tubes, sealed and degassed by nitrogen for 10 min, respectively. The reaction mixture was then irradiated under red LED strip (0.23 mW cm^{-2}) at room temperature. After different irradiation time (0, 1, 2, 3 and 6 h), the NMR tubes were transferred into the NMR instrument to collect ^{1}H NMR spectra, which are used for RAFT agent consumption calculation. For ACN insertion study, the kinetic test was almost similar, except that a molar ratio of [ACN]:[RAFT] = 10:1 was used.

Table S1. RAFT agent consumption percentages (or RAFT conversions) with various monomers at different irradiation time.

#	Monomer	[monomer] :[RAFT]	RAFT agent	Conversion at 3 h (%)	Conversion at 6 h (%)
1	PMI	1:1	**1**	2.3	3.1
2	**PMI**	**1:1**	**2**	**25.5**	**46.6**
3	**PMI**	**1:1**	**3**	**49.9**	**67.9**
4	HEMI	1:1	**1**	1.3	1.8
5	**HEMI**	**1:1**	**3**	**56.2**	**77.1**
6	ACN	1:1	**1**	3.8	6.1
7	ACN	1:1	**2**	4.1	9.3
8	ACN	1:1	**3**	8.4	14.7
9	ACN	10:1	**1**	8.0	14.8
10	**ACN**	**10:1**	**2**	**24.6**	**51.1**
11	**ACN**	**10:1**	**3**	**53.4**	**70.6**
12	MA	1:1	**1**	4.6	8.8
13	MA	1:1	**3**	7.4	12.1
14	DMA	1:1	**1**	4.6	7.4
15	DMA	1:1	**3**	6.5	10.8

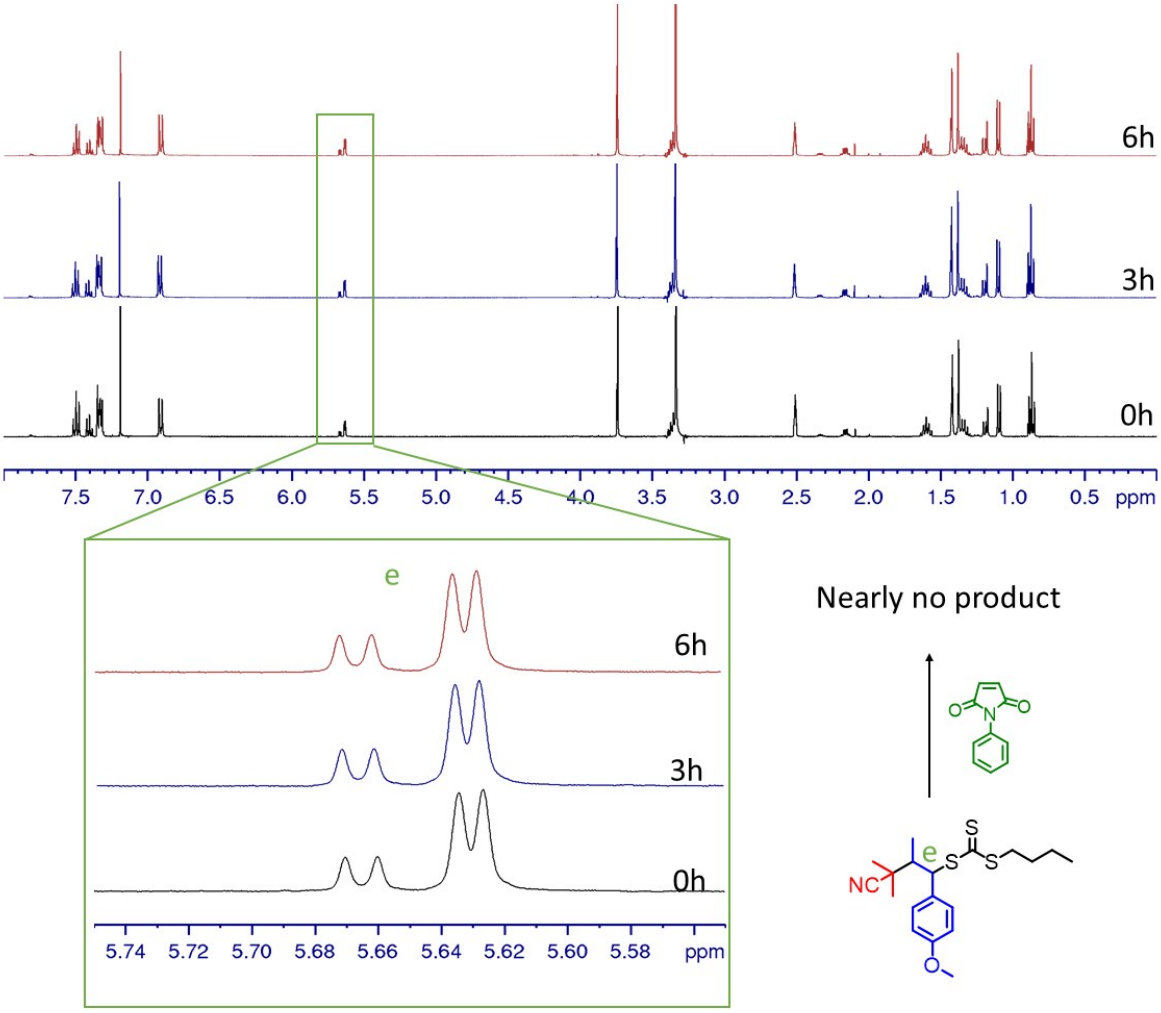

Figure S19. Stacked ^{1}H NMR (DMSO-d_6, 400 MHz) spectra at different irradiation time intervals for investigating SUMI kinetics of PMI inserted into CPBTC-Ane (**1**), indicative of negligible conversion of initial RAFT agent.

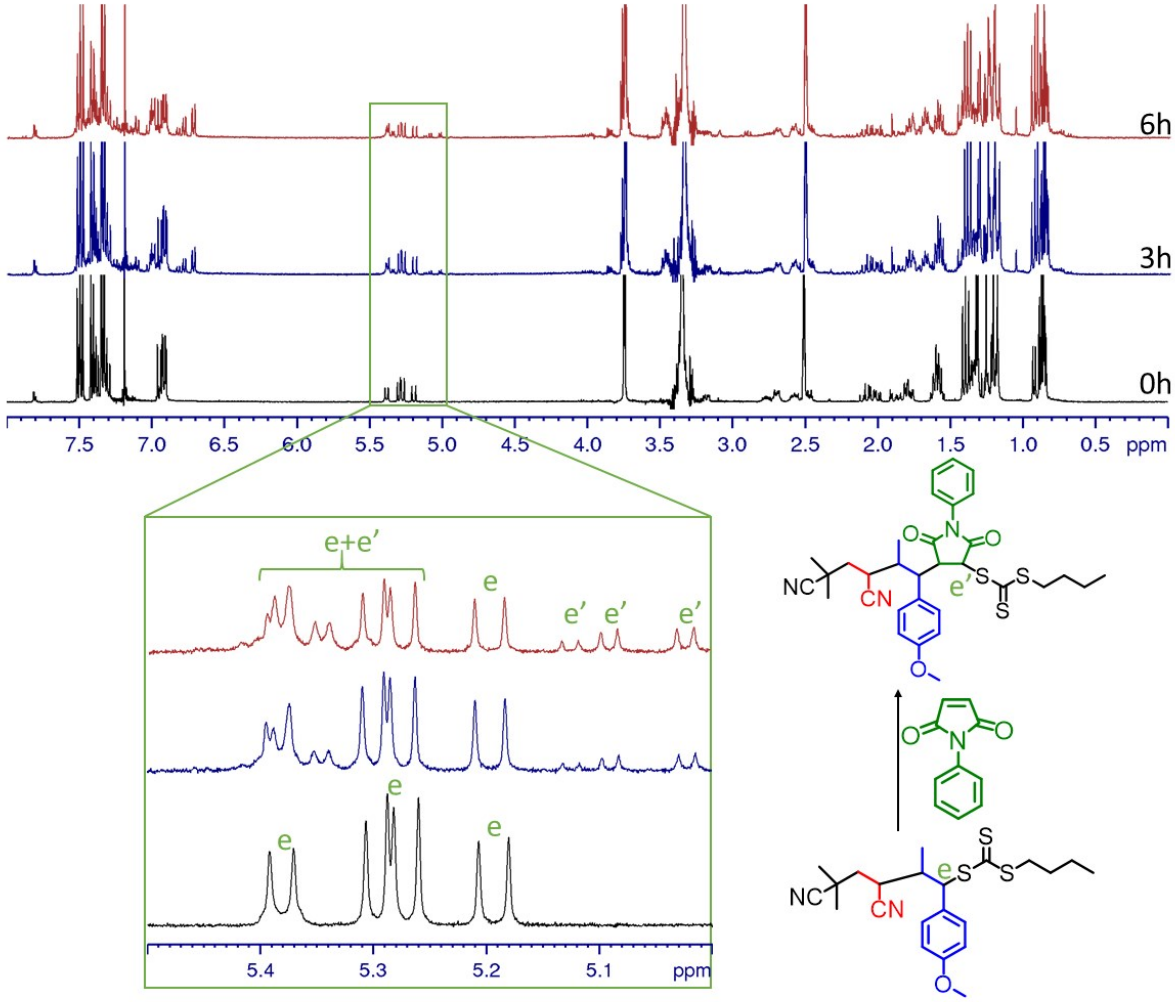

Figure S20. Stacked ^{1}H NMR (DMSO-d_6, 400 MHz) spectra at different irradiation time intervals for investigating the SUMI kinetics of PMI inserted into CPBTC-ACN-Ane (**2**), indicating effective SUMI reaction.

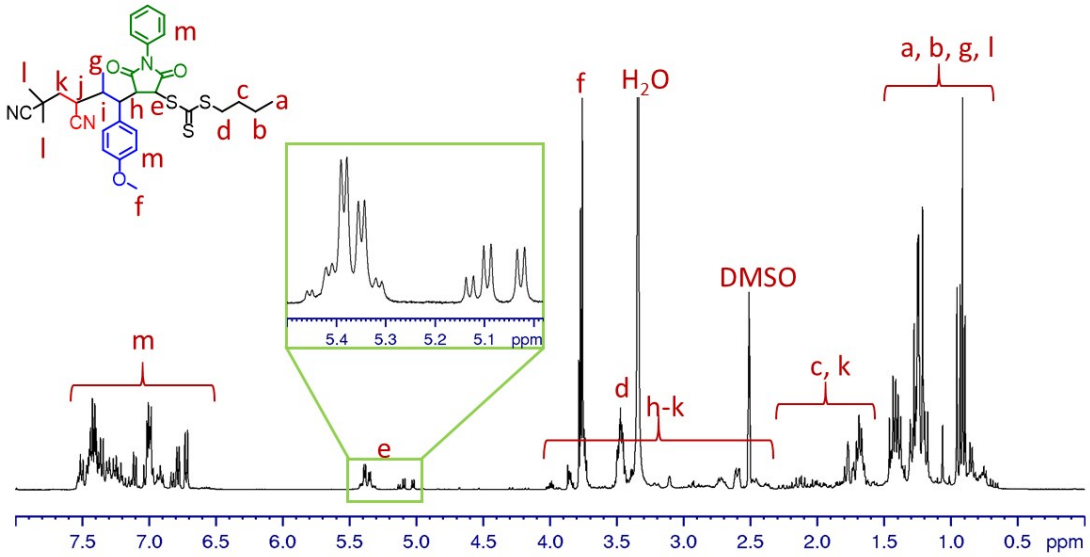

Figure S21. ^{1}H NMR (400 MHz, DMSO-d_6) of purified CPBTC-ACN-Ane-PMI.

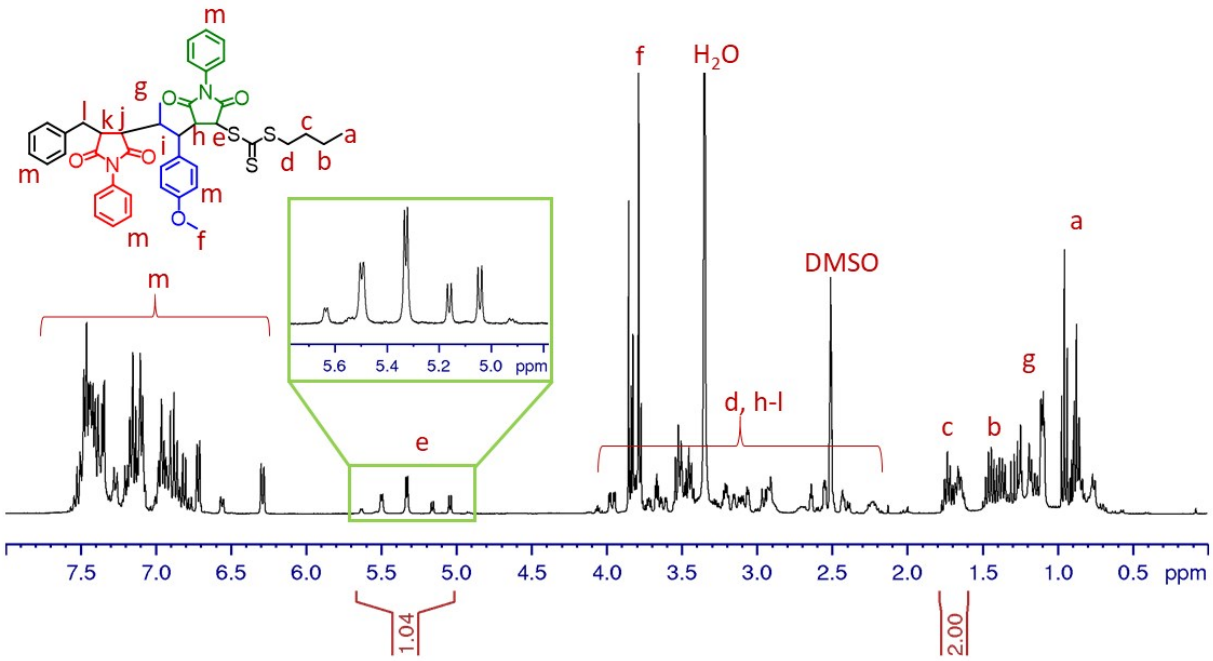

Figure S22. ^{1}H NMR (400 MHz, DMSO-d_6) of purified BBTC-PMI-Ane-PMI.

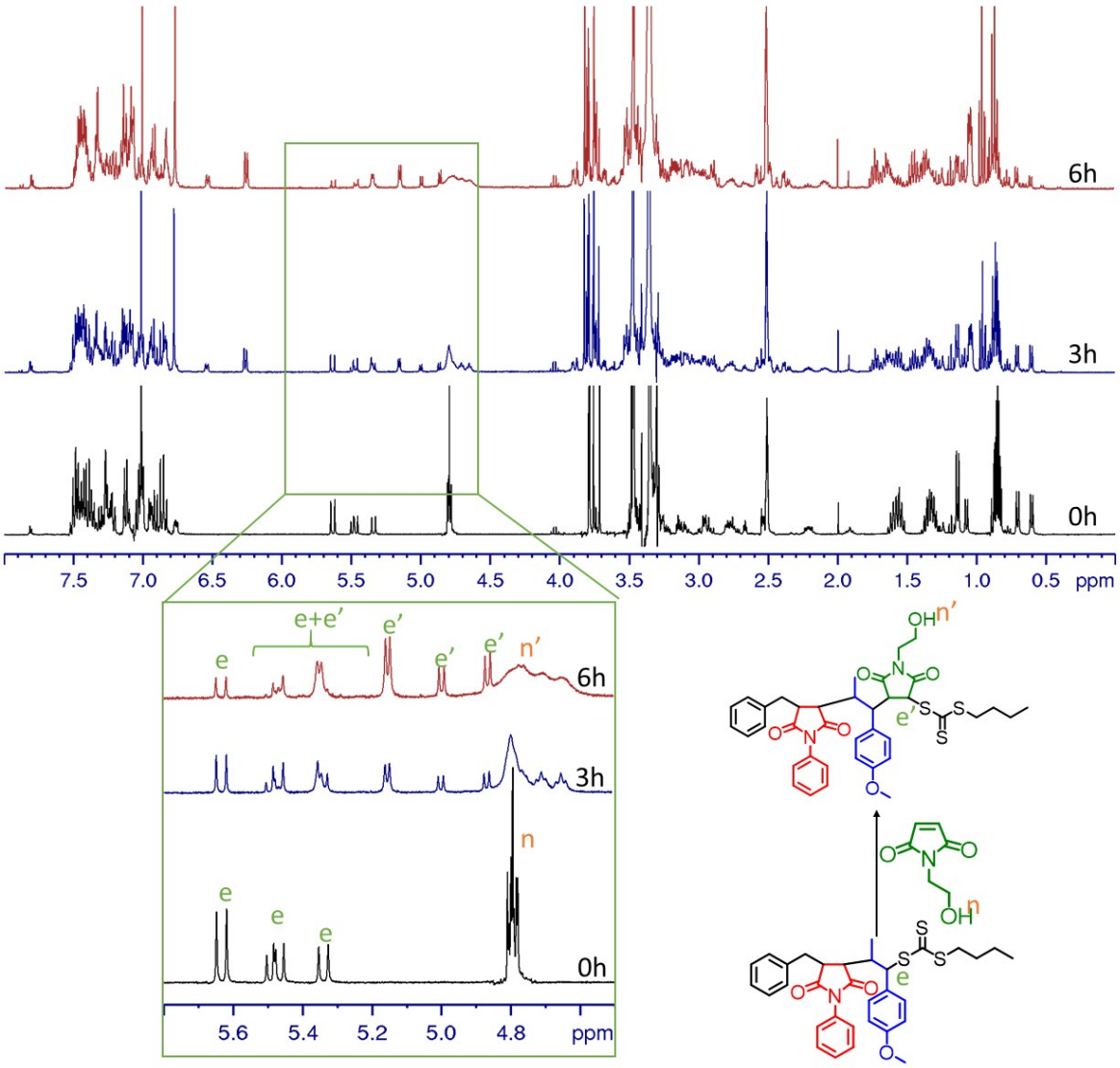

Figure S23. Stacked ^{1}H NMR (DMSO-d_6, 400 MHz) spectra at different irradiation time intervals for investigating the SUMI kinetics of HEMI inserted into BBTC-PMI-Ane (**3**), indicating effective SUMI reaction.

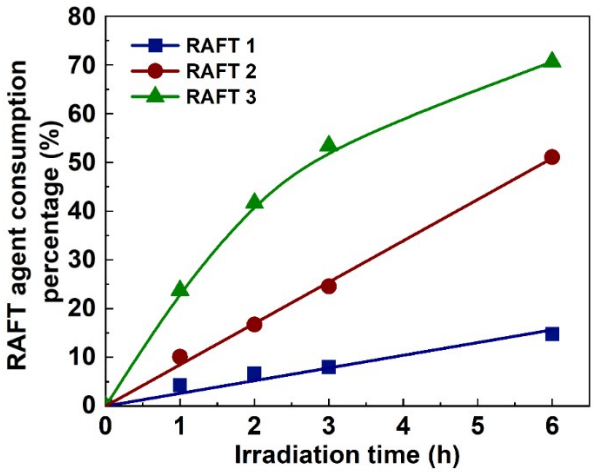

Figure S24. Kinetics of SUMI of ACN into CPBTC-Ane (**1**), CPBTC-ACN-Ane (**2**), BBTC-PMI-Ane (**3**). Reaction conditions: [ACN]:[RAFT]:[ZnTPP] = 10:1:0.01, [RAFT] = 0.025 mol L^{-1}, red light irradiation in DMSO-d_6.

4. Kinetic analysis of penultimate unit effect

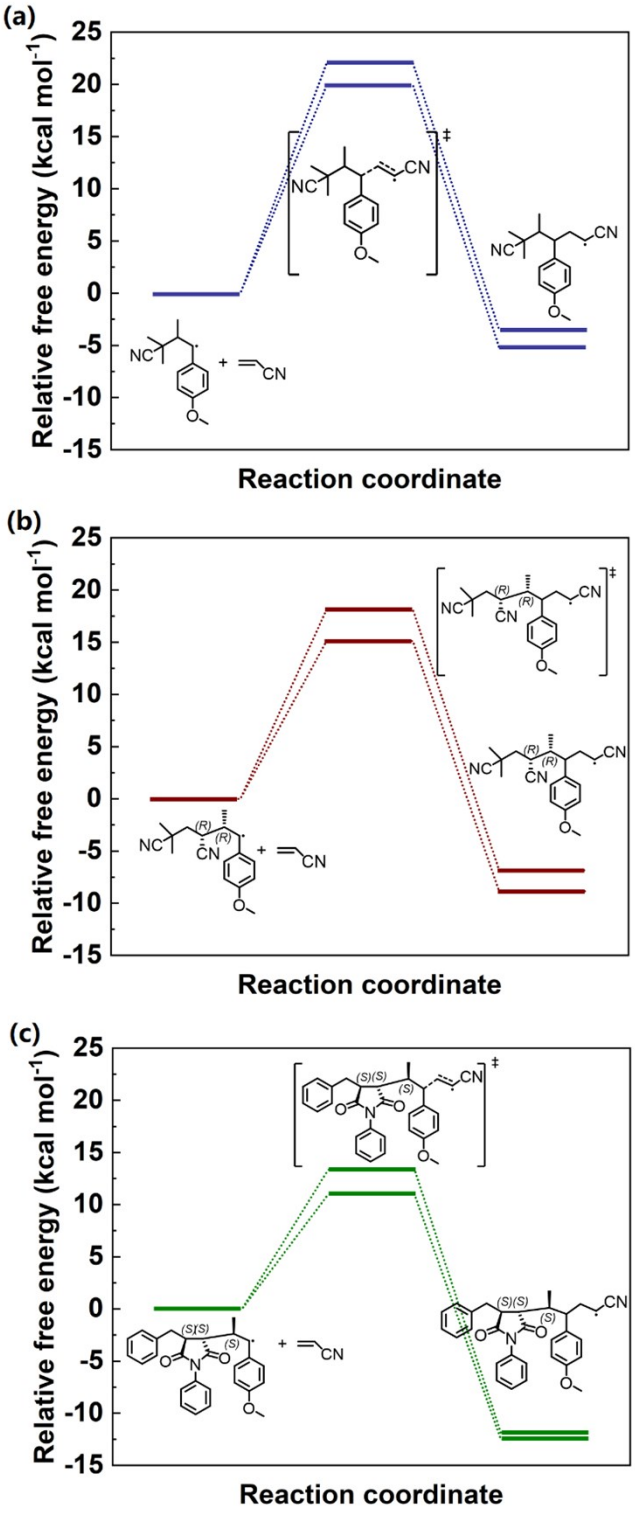

Figure S25. The potential energy surface for CPBTC-Ane (**1**), CPBTC-ACN-Ane (**2**) and BBTC-PMI-Ane (**3**) generated radicals added to ACN. *Note:* Both **2** and **3** generate two pair of enantiomeric radicals, but only the one which could lead to lower energy barrier is depicted in this Figure for comparison. Other results and more details refer to the DFT calculation at the end of this supporting document.

5. Quantum chemical calculations

Quantum chemical calculations were carried out using Gaussian 09[3]. Geometry optimization and frequency analysis of fundamental singlet and triplet (T_1) states were performed using density functional theory (DFT) at M06-2X[4]/6-31G(d)[5-9] level in gas-phase, followed by single point energy calculation at M06-2X/6-311+G(d,p)[9-12] level using SMD solvent model[13] (DMSO as solvent) at 298.15K. Thermal correction energies obtained from the frequency analysis and the above single point energy was used to calculated Gibbs free energy (*G*) and enthalpy (*H*) in DMSO.

Relaxed triplet energy of a RAFT agent ($E_{T,relaxed}$(RAFT)) was calculated by its triplet state energy (e.g. #6, T_1 CPBTC-Ane (*SS*) in **Table S2**) subtracting its ground state energy (e.g. #4, CPBTC-Ane (**1**) (*SS*) in **Table S2**). Bond dissociation energy ($D_{C\text{-}S}$) was calculated by the Gibbs free energy change (ΔG) of RAFT agents after and before photo-dissociation. Taking BBTC-PMI-Ane (*SRRR*) (**Figure S18** and **Scheme S1**) as an example, the $D_{C\text{-}S}$ was calculated as follows (the corresponding energy values are shown in #3, #37 and #45, **Table S2**):

$D_{C\text{-}S} = \Delta G = G$(R2-PMI-Ane-(*SSS*)) + G(S=C(SC_4H_9)S-) - G(BBTC-PMI-Ane (*SRRR*))

= 0.071829 Hartree = 45.07 kcal mol^{-1}

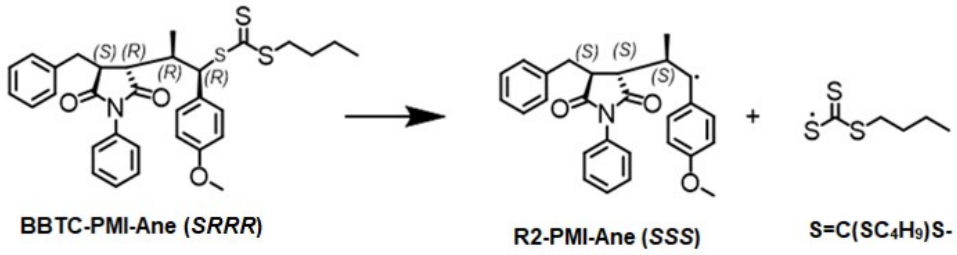

RAFT **1** with two chiral carbons has four stereoconfigurations (*RR*, *SS*, *RS*, and *SR*) with two pairs of enantiomers (*RR* and *SS vs. RS* and *SR*). It generates one pair of enantiomeric radicals (R1-Ane- (*R*) and (*S*)) that have the same radical reactivity due to their mirror images each other. Therefore, the calculation of their transition state energy barriers of addition reactions with other monomers are performed on only one enantiomeric radical, i.e., R1-Ane- (*R*) (**Scheme S1**). The other one is excluded for calculation which presents the same energy results. Similarly, both **2** and **3** generate two pairs of enantiomeric radicals and only two diastereomeric radicals for each of them are calculated (R1-ACN-Ane- (*RR*) and R1-ACN-Ane- (*RS*) radicals for **2**, and R2-PMI-Ane- (*SSS*) and R2-PMI-Ane- (*SSR*) radicals for **3** (**Scheme S1**). For clarity, the most stable configuration in four diastereomeric SUMI radicals was used for transition state energy calculation. For **1**, only one transition state was found.

However, for both **2** and **3**, two transition states for each of them were found. For ACN addition, each radical addition to ACN generates two SUMI adduct radicals, and the transition state in each path is calculated individually. So two transition states is found in RAFT **1** generate radical addition to ACN and four transition states in both **2** and **3** generated radicals addition. For PMI addition, each radical addition to PMI generates four new SUMI radicals, for simplification, each group of four new SUMI radicals were optimized firstly to find the structure with the lowest energy, as it is the most stable configuration and is supposed to be dominant in amount. The configuration with the lowest energy in each group is used for transition state calculation, and therefore only one transition state is investigated in RAFT **1** generate radical addition to PMI and two transition states in both **2** and **3** generated radicals addition.

Scheme S1. Names and structures of various species used in calculation and some related energy changes. R1 and R2 represent cyanoisopropyl and benzyl moieties, respectively.

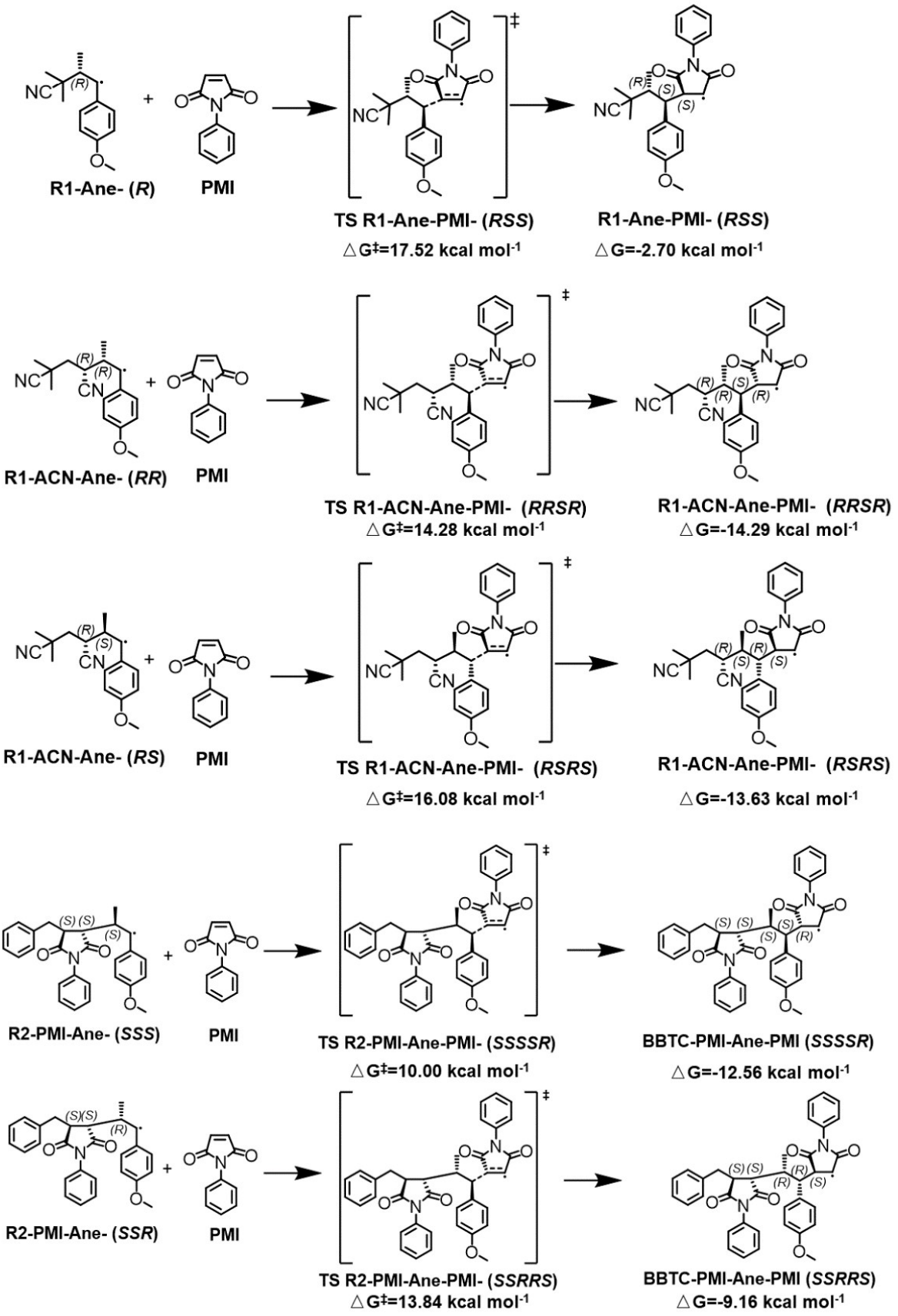

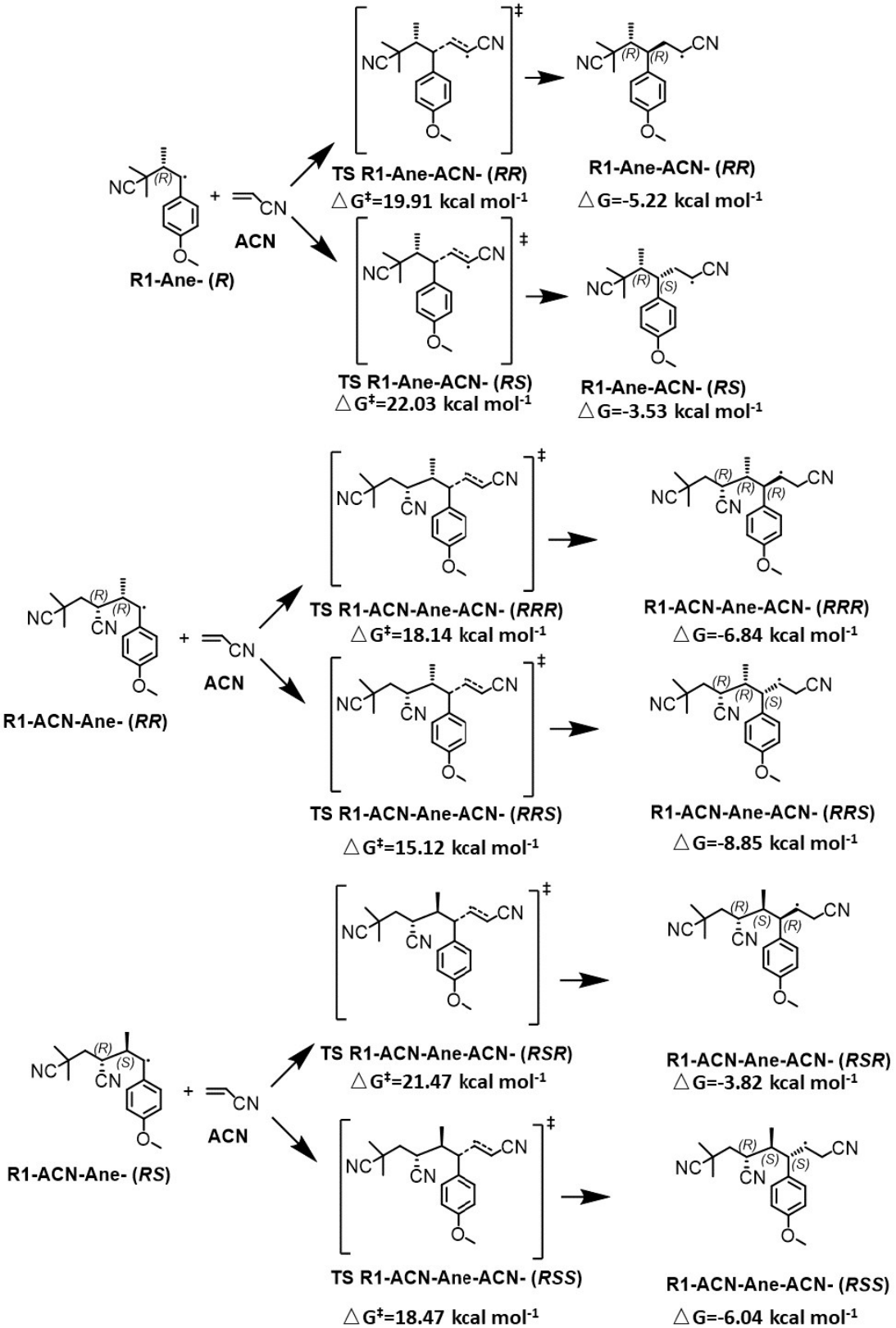
R1-Ane- (R)
ACN
TS R1-Ane-ACN- (RR)
△G‡=19.91 kcal mol-1
R1-Ane-ACN- (RR)
△G=-5.22 kcal mol-1
TS R1-Ane-ACN- (RS)
△G‡=22.03 kcal mol-1
R1-Ane-ACN- (RS)
△G=-3.53 kcal mol-1
R1-ACN-Ane- (RR)
ACN
TS R1-ACN-Ane-ACN- (RRR)
△G‡=18.14 kcal mol-1
R1-ACN-Ane-ACN- (RRR)
△G=-6.84 kcal mol-1
TS R1-ACN-Ane-ACN- (RRS)
△G‡=15.12 kcal mol-1
R1-ACN-Ane-ACN- (RRS)
△G=-8.85 kcal mol-1
R1-ACN-Ane- (RS)
ACN
TS R1-ACN-Ane-ACN- (RSR)
△G‡=21.47 kcal mol-1
R1-ACN-Ane-ACN- (RSR)
△G=-3.82 kcal mol-1
TS R1-ACN-Ane-ACN- (RSS)
△G‡=18.47 kcal mol-1
R1-ACN-Ane-ACN- (RSS)
△G=-6.04 kcal mol-1

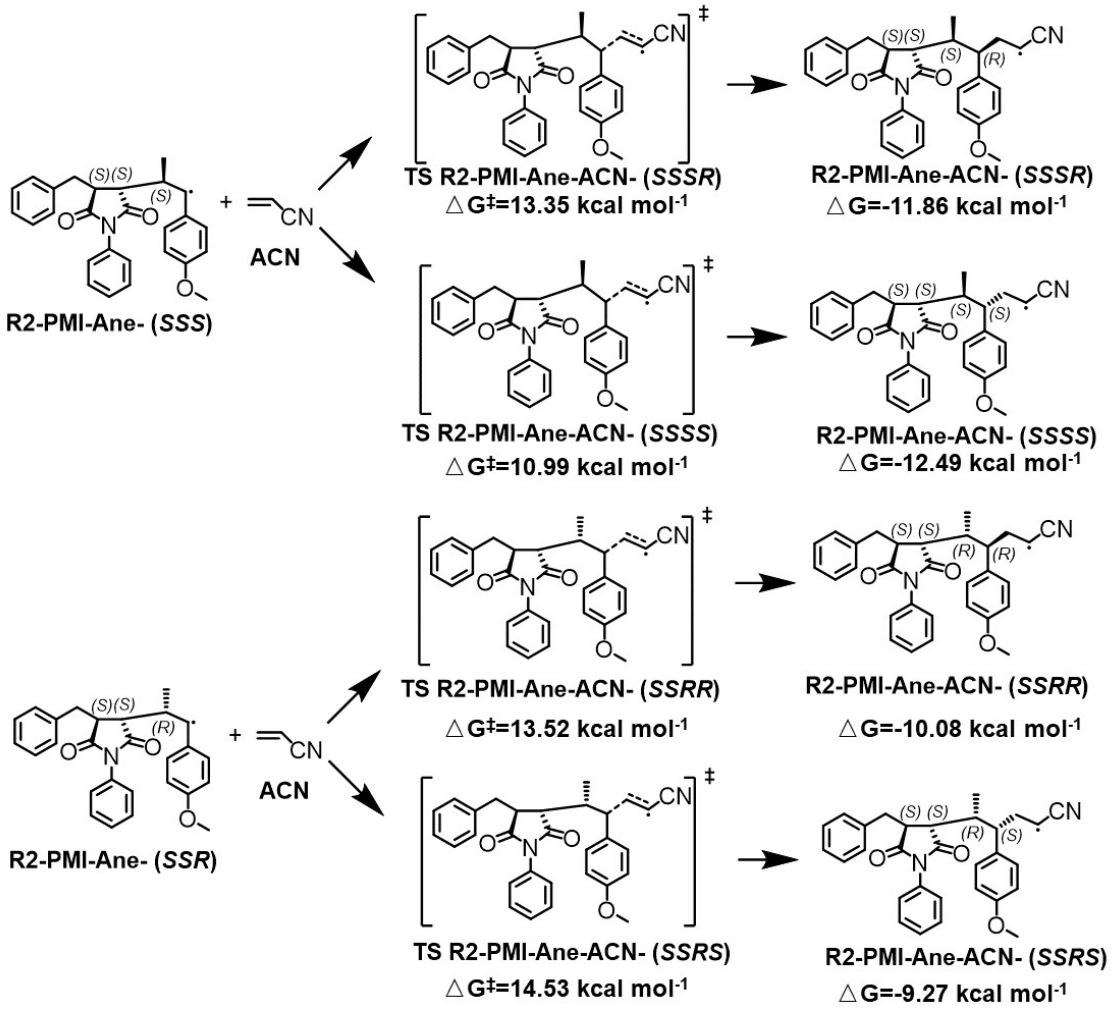
R2-PMI-Ane- (SSS)
ACN
TS R2-PMI-Ane-ACN- (SSSR)
△G‡=13.35 kcal mol-1
R2-PMI-Ane-ACN- (SSSR)
△G=-11.86 kcal mol-1
TS R2-PMI-Ane-ACN- (SSSS)
△G‡=10.99 kcal mol-1
R2-PMI-Ane-ACN- (SSSS)
△G=-12.49 kcal mol-1
R2-PMI-Ane- (SSR)
ACN
TS R2-PMI-Ane-ACN- (SSRR)
△G‡=13.52 kcal mol-1
R2-PMI-Ane-ACN- (SSRR)
△G=-10.08 kcal mol-1
TS R2-PMI-Ane-ACN- (SSRS)
△G‡=14.53 kcal mol-1
R2-PMI-Ane-ACN- (SSRS)
△G=-9.27 kcal mol-1

Table S2. Raw computational data including thermal correction energies and single point energy (Units are in Hartree.)

	Species	Correction to *H*	Correction to *G*	Single point energy	*H* in DMSO	*G* in DMSO
1	ACN	0.056727	0.025785	-170.810562	-170.753835	-170.784777
2	PMI	0.161731	0.114834	-590.422649	-590.260918	-590.307815
3	S=C(SC_4H_9)S-	0.145229	0.094756	-1390.433613	-1390.288384	-1390.338857
4	CPBTC-Ane (**1**) (*SS*)	0.459686	0.369366	-2064.665602	-2064.205916	-2064.296236
5	CPBTC-Ane (**1**) (*SR*)	0.459648	0.370902	-2064.658195	-2064.198547	-2064.287293
6	T_1 CPBTC-Ane (*SS*)[a]	0.458597	0.364433	-2064.586020	-2064.127423	-2064.221587
7	T_1 CPBTC-Ane (*SR*)[a]	0.458457	0.365639	-2064.587648	-2064.129191	-2064.222009
8	R1-Ane- (*R*)	0.309237	0.246889	-674.147727	-673.838490	-673.900838
9	R1-Ane-ACN- (*RS*)	0.370425	0.296304	-844.987540	-844.617115	-844.691236
10	R1-Ane-ACN- (*RR*)	0.370367	0.297094	-844.991023	-844.620656	-844.693929
11	TS R1-Ane-ACN- (*RS*)	0.367669	0.294971	-844.945477	-844.577808	-844.650506
12	TS R1-Ane-ACN- (*RR*)	0.367745	0.294979	-844.948864	-844.581119	-844.653885
13	R1-Ane-PMI- (*RSS*)	0.475850	0.390613	-1264.603561	-1264.127711	-1264.212948
14	TS R1-Ane-PMI- (*RSS*)	0.473225	0.388560	-1264.569291	-1264.096066	-1264.180731
15	CPBTC-ACN-Ane (**2**) (*RSS*)	0.520286	0.417785	-2235.523111	-2235.002825	-2235.105326
16	CPBTC-ACN-Ane (**2**) (*RSR*)	0.520354	0.419718	-2235.520852	-2235.000498	-2235.101134
17	CPBTC-ACN-Ane (**2**) (*RRS*)	0.520572	0.421236	-2235.522009	-2235.001437	-2235.100773
18	CPBTC-ACN-Ane (**2**) (*RRR*)	0.520562	0.419114	-2235.516653	-2234.996091	-2235.097539
19	T_1 CPBTC-ACN-Ane (*RSS*)[a]	0.519330	0.413273	-2235.445841	-2234.926511	-2235.032568
20	T_1 CPBTC-ACN-Ane (*RSR*)[a]	0.519321	0.414310	-2235.440665	-2234.921344	-2235.026355
21	T_1 CPBTC-ACN-Ane (*RRS*)[a]	0.519327	0.414722	-2235.443937	-2234.924610	-2235.029215
22	T_1 CPBTC-ACN-Ane (*RRR*)[a]	0.519508	0.413641	-2235.437111	-2234.917603	-2235.023470
23	R1-ACN-Ane- (*RR*)	0.370372	0.297344	-844.996221	-844.625849	-844.698877

24	R1-ACN-Ane- (*RS*)	0.370171	0.295753	-844.999567	-844.629396	-844.703814
25	R1-ACN-Ane-ACN- (*RRR*)	0.431042	0.348207	-1015.842760	-1015.411718	-1015.494553
26	R1-ACN-Ane-ACN- (*RRS*)	0.431448	0.348464	-1015.846221	-1015.414773	-1015.497757
27	R1-ACN-Ane-ACN- (*RSR*)	0.431714	0.348261	-1015.842946	-1015.411232	-1015.494685
28	R1-ACN-Ane-ACN- (*RSS*)	0.431190	0.346533	-1015.844752	-1015.413562	-1015.498219
29	TS R1-ACN-Ane-ACN- (*RRR*)	0.428580	0.344603	-1015.799350	-1015.370770	-1015.454747
30	TS R1-ACN-Ane-ACN- (*RRS*)	0.428598	0.345685	-1015.805238	-1015.376640	-1015.459553
31	TS R1-ACN-Ane-ACN- (*RSR*)	0.428915	0.344712	-1015.799088	-1015.370173	-1015.454376
32	TS R1-ACN-Ane-ACN- (*RSS*)	0.428355	0.343405	-1015.802563	-1015.374208	-1015.459158
33	R1-ACN-Ane-PMI- (*RRSR*)	0.536498	0.439443	-1435.463964	-1434.927466	-1435.024521
34	R1-ACN-Ane-PMI- (*RSRS*)	0.536515	0.439783	-1435.460549	-1434.924034	-1435.020766
35	TS R1-ACN-Ane-PMI- (*RRSR*)	0.534067	0.438898	-1435.427768	-1434.893701	-1434.988870
36	TS R1-ACN-Ane-PMI- (*RSRS*)	0.534027	0.439391	-1435.425398	-1434.891371	-1434.986007
37	BBTC-PMI-Ane (**3**) (*SRRR*)	0.652159	0.535307	-2715.310392	-2714.658233	-2714.775085
38	BBTC-PMI-Ane (**3**) (*SRRS*)	0.652387	0.535970	-2715.310083	-2714.657696	-2714.774113
39	BBTC-PMI-Ane (**3**) (*SRSR*)	0.652182	0.534874	-2715.298469	-2714.646287	-2714.763595
40	BBTC-PMI-Ane (**3**) (*SRSS*)	0.652151	0.535956	-2715.308582	-2714.656431	-2714.772626
41	T_1 BBTC-PMI-Ane (*SRRR*)[a]	0.651353	0.535382	-2715.231854	-2714.580501	-2714.696472
42	T_1 BBTC-PMI-Ane (*SRRS*)[a]	0.651263	0.532117	-2715.234150	-2714.582887	-2714.702033
43	T_1 BBTC-PMI-Ane (*SRSR*)[a]	0.650969	0.535135	-2715.221507	-2714.570538	-2714.686372
44	T_1 BBTC-PMI-Ane (*SRSS*)[a]	0.651111	0.530447	-2715.230148	-2714.579037	-2714.699701
45	R2-PMI-Ane- (*SSS*)	0.502292	0.414461	-1324.778860	-1324.276568	-1324.364399
46	R2-PMI-Ane- (*SSR*)	0.502425	0.414539	-1324.781898	-1324.279473	-1324.367359
47	R2-PMI-Ane-ACN- (*SSSR*)	0.562941	0.461149	-1495.629220	-1495.066279	-1495.168071
48	R2-PMI-Ane-ACN- (*SSSS*)	0.563014	0.464255	-1495.633343	-1495.070329	-1495.169088
49	R2-PMI-Ane-ACN- (*SSRR*)	0.562860	0.464515	-1495.632720	-1495.069860	-1495.168205

50	R2-PMI-Ane-ACN- (*SSRS*)	0.562914	0.462631	-1495.629534	-1495.066620	-1495.166903
51	TS R2-PMI-Ane-ACN- (SSSR)	0.560247	0.459974	-1495.587870	-1495.027623	-1495.127896
52	TS R2-PMI-Ane-ACN- (*SSSS*)	0.560232	0.460754	-1495.592419	-1495.032187	-1495.131665
53	TS R2-PMI-Ane-ACN- (*SSRR*)	0.560120	0.461009	-1495.591605	-1495.031485	-1495.130596
54	TS R2-PMI-Ane-ACN- (*SSRS*)	0.560247	0.459843	-1495.587420	-1495.027173	-1495.127577
55	R2-PMI-Ane-PMI- (*SSSSR*)	0.668591	0.557417	-1915.249644	-1914.581053	-1914.692227
56	R2-PMI-Ane-PMI- (*SSRRS*)	0.668853	0.558250	-1915.248020	-1914.579167	-1914.689770
57	TS R2-PMI-Ane-PMI- (*SSSSR*)	0.665540	0.555741	-1915.212012	-1914.546472	-1914.656271
58	TS R2-PMI-Ane-PMI- (*SSRRS*)	0.665764	0.555083	-1915.208189	-1914.542425	-1914.653106

[a]T1 means the triplet state.

References

1. Braun, D.; Hu, F., Polymers from non-homopolymerizable monomers by free radical processes. *Prog. Polym. Sci.* **2006,** *31* (3), 239-276.
2. Brandrup, J.; Immergut, E. H.; Grulke, E. A.; Abe, A.; Bloch, D. R., *Polymer handbook*. Wiley New York: 1999; Vol. 89.
3. Frisch, M. J.; Trucks, G. W.; Schlegel, H. B.; Scuseria, G. E.; Robb, M. A.; Cheeseman, J. R.; Scalmani, G.; Barone, V.; Petersson, G. A.; Nakatsuji, H.; Li, X.; Caricato, M.; Marenich, A. V.; Bloino, J.; Janesko, B. G.; Gomperts, R.; Mennucci, B.; Hratchian, H. P.; Ortiz, J. V.; Izmaylov, A. F.; Sonnenberg, J. L.; Williams; Ding, F.; Lipparini, F.; Egidi, F.; Goings, J.; Peng, B.; Petrone, A.; Henderson, T.; Ranasinghe, D.; Zakrzewski, V. G.; Gao, J.; Rega, N.; Zheng, G.; Liang, W.; Hada, M.; Ehara, M.; Toyota, K.; Fukuda, R.; Hasegawa, J.; Ishida, M.; Nakajima, T.; Honda, Y.; Kitao, O.; Nakai, H.; Vreven, T.; Throssell, K.; Montgomery Jr., J. A.; Peralta, J. E.; Ogliaro, F.; Bearpark, M. J.; Heyd, J. J.; Brothers, E. N.; Kudin, K. N.; Staroverov, V. N.; Keith, T. A.; Kobayashi, R.; Normand, J.; Raghavachari, K.; Rendell, A. P.; Burant, J. C.; Iyengar, S. S.; Tomasi, J.; Cossi, M.; Millam, J. M.; Klene, M.; Adamo, C.; Cammi, R.; Ochterski, J. W.; Martin, R. L.; Morokuma, K.; Farkas, O.; Foresman, J. B.; Fox, D. J. *Gaussian 09 Rev. D.01*, Wallingford, CT, 2013.
4. Zhao, Y.; Truhlar, D. G., The M06 suite of density functionals for main group thermochemistry, thermochemical kinetics, noncovalent interactions, excited states, and transition elements: two new functionals and systematic testing of four M06-class functionals and 12 other functionals. *Theor. Chem. Acc.* **2008,** *120* (1-3), 215-241.
5. Ditchfield, R.; Hehre, W. J.; Pople, J. A., Self-consistent molecular-orbital methods. IX. An extended Gaussian-type basis for molecular-orbital studies of organic molecules. *The Journal of Chemical Physics* **1971,** *54* (2), 724-728.
6. Hehre, W. J.; Ditchfield, R.; Pople, J. A., Self—consistent molecular orbital methods. XII. Further extensions of Gaussian—type basis sets for use in molecular orbital studies of organic molecules. *The Journal of Chemical Physics* **1972,** *56* (5), 2257-2261.
7. Hariharan, P. C.; Pople, J. A., The influence of polarization functions on molecular orbital hydrogenation energies. *Theor. Chim. Acta* **1973,** *28* (3), 213-222.
8. Gordon, M. S.; Binkley, J. S.; Pople, J. A.; Pietro, W. J.; Hehre, W., Self-consistent molecular-orbital methods. 22. Small split-valence basis sets for second-row elements. *J Journal of the American Chemical Society* **1982,** *104* (10), 2797-2803.
9. Francl, M. M.; Pietro, W. J.; Hehre, W. J.; Binkley, J. S.; Gordon, M. S.; DeFrees, D. J.; Pople, J. A., Self-consistent molecular orbital methods. XXIII. A polarization-type basis set for second-row elements. *The Journal of Chemical Physics* **1982,** *77* (7), 3654-3665.
10. Krishnan, R.; Binkley, J. S.; Seeger, R.; Pople, J. A., Self-consistent molecular orbital methods. XX. A basis set for correlated wave functions. *The Journal of Chemical Physics* **1980,** *72* (1), 650-654.
11. Clark, T.; Chandrasekhar, J.; Spitznagel, G. W.; Schleyer, P. V. R., Efficient diffuse function-augmented basis sets for anion calculations. III. The 3-21+ G basis set for first-row elements, Li–F. *J. Comput. Chem.* **1983,** *4* (3), 294-301.
12. Spitznagel, G. W.; Clark, T.; von Ragué Schleyer, P.; Hehre, W., An evaluation of the performance of diffuse function-augmented basis sets for second row elements, Na-Cl. *J. Comput. Chem.* **1987,** *8* (8), 1109-1116.
13. Marenich, A. V.; Cramer, C. J.; Truhlar, D. G., Universal solvation model based on solute electron density and on a continuum model of the solvent defined by the bulk

dielectric constant and atomic surface tensions. *The Journal of Physical Chemistry B* **2009,** *113* (18), 6378-6396.